

See discussions, stats, and author profiles for this publication at: <https://www.researchgate.net/publication/44657953>

A new family of oxime-based hexanuclear manganese(III) single molecule magnets with high anisotropy energy barriers

ARTICLE *in* CHEMICAL COMMUNICATIONS · JULY 2010

Impact Factor: 6.83 · DOI: 10.1039/c0cc00485e · Source: PubMed

CITATIONS

27

READS

25

12 AUTHORS, INCLUDING:



José Martínez-Lillo

University of Valencia

40 PUBLICATIONS 546 CITATIONS

SEE PROFILE



Eduard Cremades

University of Barcelona

22 PUBLICATIONS 1,430 CITATIONS

SEE PROFILE



Eliseo Ruiz

University of Barcelona

205 PUBLICATIONS 7,996 CITATIONS

SEE PROFILE



Verdaguer Michel

Pierre and Marie Curie University - Paris 6

122 PUBLICATIONS 7,474 CITATIONS

SEE PROFILE

A new family of oxime-based hexanuclear manganese(III) single molecule magnets with high anisotropy energy barriers†

Adrian-Raul Tomsa,^{‡a} José Martínez-Lillo,^a Yanling Li,^a Lise-Marie Chamoreau,^a Kamal Boubekeur,^a Fernanda Farias,^b Miguel A. Novak,^b Eduard Cremades,^c Eliseo Ruiz,^c Anna Proust,^{ad} Michel Verdaguer^{*a} and Pierre Gouzerh^{*a}

Received 19th March 2010, Accepted 13th May 2010

First published as an Advance Article on the web 7th June 2010

DOI: 10.1039/c0cc00485e

A magneto-structural study of two salicylamidoxime-based {Mn₆} single-molecule magnets revealed that their anisotropy energy barriers, which can reach the current record for *d*-transition metal complexes, are strongly dependent upon the precise arrangement of ligands and the solvation state.

Since their first report in 2004,¹ oxime-based hexanuclear Mn^{III} clusters of general formula [Mn^{III}₆O₂(X-sao)₆(O₂CR)₂·(Solvent)_{*n*}] (H-saoH₂ = salicylaldoxime; X = H, Me, Et; R = alkyl or aryl; Solvent = H₂O, MeOH, EtOH; *n* = 4–6) have emerged as a versatile class of single-molecule magnets (SMMs). They are made of two symmetry-equivalent {Mn^{III}₃(μ₃-O)} triangular moieties linked *via* phenolate and oximate oxygen atoms, with long axial bonds roughly aligned perpendicular to the Mn^{III}₃ planes. While the inter-triangle magnetic exchange is in most cases ferromagnetic, the intra-triangle magnetic exchange can be either antiferromagnetic or ferromagnetic, resulting in *S* = 4 or *S* = 12 ground states, respectively. Ferromagnetic exchange in oxime-based {Mn^{III}₃(μ₃-O)} triangles largely originates from twisting of the oxime ligands resulting in large Mn–N–O–Mn torsion angles.^{2–5} Accordingly, the deliberate structural distortion of the {Mn₆} molecule allowed the change of the intra-triangle magnetic exchange from antiferromagnetic to ferromagnetic, thus enhancing the effective energy barrier for magnetization reversal to record levels.^{3,4} The magnitude of the ground state magnetic anisotropy has been addressed theoretically.⁶

In continuity of our long-standing interest in amidoxime ligands,⁷ we recently looked into the chemistry of salicylamidoxime (H₂N-saoH₂) with manganese to explore if the preceding record barriers can be reached with different equatorial ligands. We have characterized several {Mn₆} clusters whose main features appear similar to those of clusters formed by

derivatized salicylaldoximes (X = Me, Et) but allow to point out new factors that determine magnetic properties.

Two different compounds, [Mn₆O₂(H₂N-sao)₆·(PhCO₂)₂(EtOH)₄(H₂O)₂·8EtOH (**1**) and [Mn₆O₂(H₂N-sao)₆·(PhCO₂)₂(EtOH)₆]·EtOH·H₂O (**2**) were obtained by reaction of Mn(II) chloride with salicylamidoxime and sodium benzoate in ethanol.[§] Both compounds were characterized by elemental analysis, IR spectroscopy, single-crystal X-ray diffraction,[¶] and SQUID magnetometry.^{||} While they have close compositions and nearly identical IR spectra, they display quite different magnetic properties which have been correlated to significant differences in their molecular structures.

The {Mn₆} cluster in **1** consists of two {Mn^{III}₃(μ₃-O)(H₂N-sao)₃}⁺ subunits linked together *via* two pairs of long Mn–O bonds involving two oximate oxygen atoms and two phenolate oxygen atoms. Each Mn centre achieves six-coordination with axial benzoate and/or solvent ligands. The axial benzoate ligand is *trans* to a solvent molecule, that defines a structural type *a* (Fig. 1). While the molecular structure of **1** is broadly similar to those of other oxime-based {Mn₆} clusters,^{1,3–6} the actual combination and arrangement of ligands are rarely encountered.

In **2**, the unit cell contains two chemically equivalent and crystallographically independent {Mn₆} clusters, the molecular structure of one of them is shown in Fig. 1. The basic framework of the {Mn₆} complexes is maintained but a significant

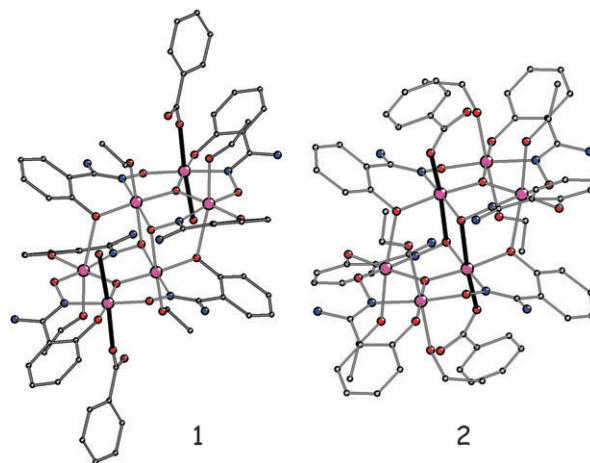


Fig. 1 Molecular structures of the {Mn₆} clusters in **1** and **2**, highlighting the difference between structural types *a* (**1**: benzoate *trans* to H₂O) and *b* (**2**: benzoate *trans* to oximate). Colour code: Mn, purple; O, red; N, blue; C, black.

^a Institut Parisien de Chimie Moléculaire, UMR CNRS 7201, Case courrier 42, Université Pierre et Marie Curie Paris 6, Place Jussieu, 75252 Paris Cedex 05, France.

E-mail: michel.verdaguer@upmc.fr, pierre.gouzerh@upmc.fr

^b Instituto de Física, Universidade Federal de Rio de Janeiro, Rio de Janeiro-RJ, 21945-970, Brazil

^c Departament de Química Inorgànica and Institut de Recerca en Química Teòrica i Computacional, Universitat de Barcelona, Diagonal 647, 08028, Barcelona, Spain

^d Institut Universitaire de France, France

† Electronic supplementary information (ESI) available: Fig. S1–S10. CCDC 769840 and 769841. For ESI and crystallographic data in CIF or other electronic format see DOI: 10.1039/c0cc00485e

‡ Current address: “Raluca Ripan” Institute for Research in Chemistry, 30 Fantanele St. RO-400294 Cluj-Napoca, Romania.

difference between the clusters in **1** and **2** lies in the position of the benzoate ligands, located *trans* to the oximate oxygen atom that links the Mn^{III}₃ triangles in **2**, which defines structural type *b*. A direct consequence is that the Mn–N–O–Mn torsion angles in **2** are much higher than for **1** (See Table 1). As regards the link between the {Mn^{III}₃} subunits in the two clusters in **2** (see footnote †), the oximate bridges (Mn–O = 2.35(1) Å, O–Mn–O = 82.9(4)°; Mn–O = 2.35(1) Å, O–Mn–O = 82.0(4)°) are similar to the one in **1** (Mn–O = 2.377(2) Å, O–Mn–O = 84.4(9)°), while the distances to phenolate oxygen atoms (Mn–O = 2.44(1) Å and 2.42(1) Å are significantly shorter than in **1** (2.675(2) Å).

Plots of $\chi_M T$ vs. T for **1** and **2** are shown in Fig. 2.

For **1**, they clearly reflect intra-triangle antiferromagnetic exchange and a $S = 4$ ground state, shown also by the magnetization $M/N\mu_B$ vs H/T (Fig. S1†). The opening of an hysteresis loop at 1.8 K (Fig. S2†) and the *ac* susceptibility (Fig. S3†) are consistent with SMM behaviour. A striking point is that the *ac* properties depend on the history of the sample. When the crystals picked from the mother solution are quickly dried and introduced in the SQUID at 200 K only one fast relaxation process is present (Fig. S3†). When **1** is partially desolvated, the plots of out-of-phase χ_M'' *ac* susceptibility vs T show two maxima, which demonstrates the presence of two species having one fast and one slow relaxation process. Introduction and purge at 300 K in the locking-chamber of the SQUID resulted in a significant increase of the slowly relaxing species (Fig. 3a). Anisotropy energy barriers of 24 and 86 K were calculated from Arrhenius plots for the two relaxation processes (Fig. S3 and S4†). The obvious explanation is that **1** presents a spin $S = 4$ ground state and $U_{\text{eff}} = 24$ K and that a slight increase of the torsion angles induced by (partial) desolvation transforms part of the molecules in a spin $S = 12$ ground state SMM with $U_{\text{eff}} = 86$ K.

As for **2**, plots of $\chi_M T$ vs. T (Fig. 2) and of the magnetization $M/N\mu_B$ vs H/T (Fig. S5†) support a ground spin state close to 12. The hysteresis loop of the magnetization indicates a significant quantum tunneling effect at zero-field (Fig. S6†), as already observed in salicylaldoxime-based {Mn₆} clusters.^{3d} Double-peaked frequency-dependent χ_M' and χ_M'' *ac* susceptibilities are seen below 10 K with similar intensity (Fig. 3b) as

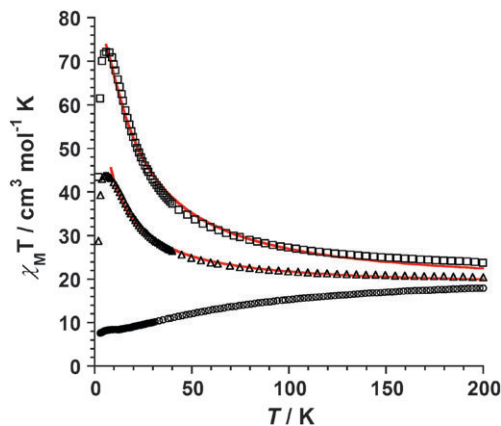


Fig. 2 Thermal variation of the molar susceptibility of **1** (o), **2** (Δ) and **2'** (□) (see text) as the $\chi_M T$ product. Also shown are the fitting curves for **2** and **2'** (see Table 2).

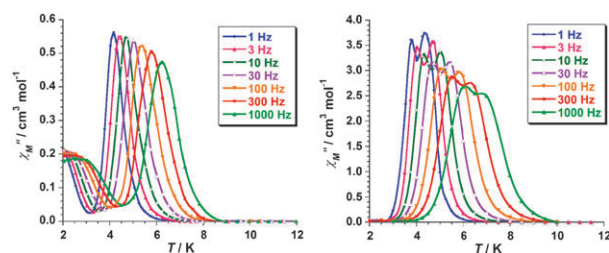


Fig. 3 Out-of-phase susceptibility (χ_M'') in the 2–12 K and 1–1000 Hz ranges for samples of **1** (a, left) and of **2** (b, right) (see text).

expected from the presence of two independent different clusters in a 1:1 ratio. The corresponding energy barriers are 68 and 86 K (Fig. S7†).

Various batches of **2** have been obtained in the search for crystals with better X-ray quality. While they have similar habit and quite similar cell parameters, their magnetic properties show some variability which may reflect small differences in the structural parameters of the individual clusters. Fig. 2 and the supplementary material† include data for a sample (**2'**) for which no structure is available.

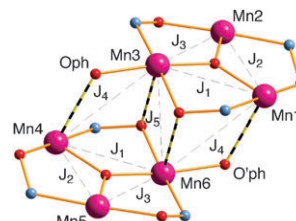
We have performed electronic structure calculations using density functional theory (see ref. 8a–d) to calculate the sets of exchange coupling constants defined in Hamiltonian (1) and Scheme 1, for the three molecules in **1** and **2** (Table 1).

$$\hat{H} = -2J_1[\hat{S}_1\hat{S}_3 + \hat{S}_4\hat{S}_6] - 2J_2[\hat{S}_1\hat{S}_2 + \hat{S}_4\hat{S}_5] - 2J_3[\hat{S}_2\hat{S}_3 + \hat{S}_5\hat{S}_6] - 2J_4[\hat{S}_3\hat{S}_4 + \hat{S}_1\hat{S}_6] - 2J_5\hat{S}_3\hat{S}_6 \quad (1)$$

Table 1 Calculated exchange coupling constants J_1 – J_5 and total spin of the ground state in **1** and **2**, using the B3LYP functional^{8e} and all electron triple- ζ basis set^{8f} using Gaussian03,^{8g} together with experimental Mn–N–O–Mn torsion angles

Complex	Mn–N–O–Mn/°	J_1 – J_5/cm^{-1}	S_{calcd}
1	38.5(3), 28.9(3), 29.5(3)	–1.1, +1.9, +1.6 –1.2, +2.9	1
2	47(1), 38(1), 34(1)	+3.4, +0.6, +1.7	12
(see†)	49(1), 38(1), 32(1)	–0.1, +3.5 +3.0, +1.1, +2.7 +0.2, +3.7	12

The results are in line with the structural and magnetic data (inter-triangle ferromagnetic coupling, due to the dominant central ferromagnetic J_5 constant, intra-triangle antiferromagnetic coupling for small torsion angles in **1**, and intra-triangle ferromagnetic for large angles in **2**). The calculated spin of the ground state in **1** is $S = 1$ but there are many states with S values between 0 and 4 very close in energy.



Scheme 1 Coupling constants numbering

Table 2 Fitted magnetic parameters for **1**, **2** and **2'**

Complex	J_1 – J_5/cm^{-1}	S^a	g^a	D/cm^{-1a}	$U_{\text{eff}}/\text{K}^b$
1	n.a.	4	1.99	–1.55	24/86
2	+2.4, +1.1, +1.1 –1.3, +3.4	11	2.01	–0.50	68/86
2'	+8.2, +1.2, +1.1 –0.4, +1.4	12	2.00	–0.41	68/86

^a From fit of magnetization measurements (Anisofit2.0 program).

^b From *ac* susceptibility measurements (see text); n.a. = not available. (see ESI).

The calculated J values were employed as a starting set to perform the fitting of the experimental magnetic susceptibility of **1**, **2** and **2'**. The fitted J values are collected in Table 2. While it was impossible to fit the magnetic susceptibility of **1** with realistic values as for some other $S = 4$ systems,^{1,3e} good fits were obtained for **2** and **2'** (Fig. 2).

In summary our results show that: (i) the {Mn₆} SMM series discovered by Milios and Brechin can be extended to salicylamidoxime derivatives, with equalled anisotropy barriers; (ii) two structural types, *a* and *b*, can be defined; type *a* is related to $S = 4$ and small anisotropy barriers; type *b* is most often associated to $S = 12$ and large barriers; a third type, *c*, where the carboxylate is *trans* to phenolate oxygen atoms, not involved here, will be reported in a forthcoming publication; clusters with bridging carboxylates, *trans* to phenolate and oximate oxygen, represent a fourth type; (iii) the compounds and their magnetic properties are very sensitive to (de)solvation processes; (iv) high spin and high energy barrier ground state, consequence of large Mn–N–O–Mn equatorial torsion angles, can arise not only from increased ligand bulkiness,^{3,4} but also from the precise arrangement of ligands (type *b* vs. type *a*) and in type *a* structures, from a solvation–reorganization process.

This work was supported by UPMC through a postdoctoral grant (ART) and by the CNRS, by Ministerio de Ciencia e Innovación through the project CTQ2008-06670-C02-01, a postdoctoral grant (JML) and a FPI predoctoral grant (EC), by Generalitat de Catalunya (2009SGR-1459), and by CNPq and FAPERJ (Brazil). The authors thankfully acknowledge the computer resources of *Centre de Supercomputació de Catalunya*.

Notes and references

§ Synthesis of **1**: MnCl₂·4H₂O (0.30 g, 1.5 mmol) dissolved in EtOH (25 mL) was added to a refluxing solution of salicylamidoxime (0.24 g, 1.6 mmol), benzoic acid (0.55 g, 4.5 mmol) and sodium carbonate (0.238 g, 2.2 mmol) in EtOH (50 mL). The resulting brown–green mixture was refluxed for 6 h and then cooled to room temperature. The solution was filtered and allowed to stand for 2 weeks. Brown–green crystals formed, which were suitable for structural analysis (**1**). They were collected by suction filtration, washed with 2 mL EtOH, and dried in air. Yield: 0.24 g (56% based on Mn). Anal. Calcd. (Found) for C₆₄H₇₄Mn₆N₁₂O₂₄: N 9.74 (10.28), Mn 19.11 (19.58).

Synthesis of **2**: A mixture of sodium benzoate (6 g, 41.6 mmol), salicylamidoxime (2.4 g, 15.8 mmol) and MnCl₂·4H₂O (2.96 g, 15 mmol) in 750 mL 95% EtOH was refluxed for 5 h. The reaction mixture was cooled to room temperature and filtered. A brown–green microcrystalline solid (**2**) formed within a few days. Yield: 1.95 g (42% based on Mn). Calcd. (Found) for C₇₀H₉₀Mn₆N₁₂O₂₆: N 9.11 (8.98), Mn 17.86 (18.12). Several batches of crystals of **2** were obtained in the course of repeated attempts to get crystals suitable for structural analysis.

¶ Crystal data for **1**: $M = 2093.54 \text{ g mol}^{-1}$, C₈₀H₁₂₂Mn₆N₁₂O₃₂, space group $P\bar{1}$, $a = 12.4800(14)$, $b = 14.0040(15)$, $c = 16.3390(16) \text{ Å}$, $\alpha = 81.632(8)$, $\beta = 69.687(9)$, $\gamma = 65.125(8)^\circ$, $V = 2429.5(5) \text{ Å}^3$, $T = 250 \text{ K}$, $Z = 1$, $\rho = 1.43 \text{ g cm}^{-3}$, $R_{\text{int}} = 0.0464$, $R = 0.0553$ for 7681 reflections with $I > 2\sigma(I)$, $R = 0.1016$ for all reflections. Crystal data for **2**: $M = 1845.18 \text{ g mol}^{-1}$, C₇₀H₉₀Mn₆N₁₂O₂₆, space group $P\bar{1}$, $a = 13.388(3)$, $b = 13.497(4)$, $c = 24.781(9) \text{ Å}$, $\alpha = 104.97(2)$, $\beta = 94.08(3)$, $\gamma = 103.10(2)^\circ$, $V = 4173(2) \text{ Å}^3$, $T = 200 \text{ K}$, $Z = 2$, $\rho = 1.47 \text{ g cm}^{-3}$, $R_{\text{int}} = 0.0544$, $R = 0.152$ for 10016 reflections with $I > 2\sigma(I)$, $R = 0.175$ for all reflections. This structure was refined to a rather low level due to the poor quality of the crystals. Intensity data were collected with a Bruker-Nonius Kappa-CCD with graphite-monochromated Mo-K α radiation. Unit-cell parameters determination, data collection strategy and integration were carried out with the Nonius EVAL-14 suite of programs. Multi-scan absorption correction was applied. The structures were solved by direct methods using SHELXS-97 and refined by full-matrix least-squares methods using the SHELXL-97 software package.^{9a,b} All non hydrogen atoms were refined anisotropically. CCDC 769840 and 769841.

|| Magnetization was measured (i) in the 2–300 K or 2–200 K range, applying 0.1 T magnetic induction, (ii) in the 2–10 K and 2–7 T range, *ac* susceptibility measurements were performed in the 2–12 K range, in zero applied *dc* field and a $3 \cdot 10^{-4} \text{ T}$ *ac* field oscillating at 1–1000 Hz.

- 1 C. J. Milios, C. P. Raptopoulou, A. Terzis, F. Lloret, R. Vicente, S. P. Perlepes and A. Escuer, *Angew. Chem., Int. Ed.*, 2004, **43**, 210–212.
- 2 (a) T. C. Stamatatos, D. Foguet-Albiol, S.-C. Lee, C. C. Stoumpos, C. P. Raptopoulou, A. Terzis, W. Wernsdorfer, S. O. Hill, S. P. Perlepes and G. Christou, *J. Am. Chem. Soc.*, 2007, **129**, 9484–9499; (b) J. Cano, T. Cauchy, E. Ruiz, C. J. Milios, C. C. Stoumpos, T. C. Stamatatos, S. P. Perlepes, G. Christou and E. K. Brechin, *Dalton Trans.*, 2008, 234–240; (c) C.-I. Yang, W. Wernsdorfer, K.-H. Cheng, M. Nakano, G.-H. Lee and H.-L. Tsai, *Inorg. Chem.*, 2008, **47**, 10184–10186.
- 3 (a) C. J. Milios, A. Vinslava, P. A. Wood, S. Parsons, W. Wernsdorfer, G. Christou, S. P. Perlepes and E. K. Brechin, *J. Am. Chem. Soc.*, 2007, **129**, 8–9; (b) C. J. Milios, A. Vinslava, W. Wernsdorfer, S. Moggach, S. Parsons, S. P. Perlepes, G. Christou and E. K. Brechin, *J. Am. Chem. Soc.*, 2007, **129**, 2754–2755; (c) C. J. Milios, A. Vinslava, W. Wernsdorfer, A. Prescimone, P. A. Wood, S. Parsons, S. P. Perlepes, G. Christou and E. K. Brechin, *J. Am. Chem. Soc.*, 2007, **129**, 6547–6561; (d) C. J. Milios, R. Inglis, R. Bagai, W. Wernsdorfer, A. Collins, S. Moggach, S. Parsons, S. P. Perlepes, G. Christou and E. K. Brechin, *Chem. Commun.*, 2007, 3476–3478; (e) C. J. Milios, R. Inglis, A. Vinslava, R. Bagai, W. Wernsdorfer, S. Parsons, S. P. Perlepes, G. Christou and E. K. Brechin, *J. Am. Chem. Soc.*, 2007, **129**, 12505–12511.
- 4 C. J. Milios, S. Piligkos and E. K. Brechin, *Dalton Trans.*, 2008, 1809–1817(Perspective).
- 5 R. Inglis, L. F. Jones, C. J. Milios, S. Datta, A. Collins, S. Parsons, W. Wernsdorfer, S. Hill, S. P. Perlepes, S. Piligkos and E. K. Brechin, *Dalton Trans.*, 2009, 3403–3412.
- 6 (a) E. Ruiz, J. Cirera, J. Cano, S. Alvarez, C. Loose and J. Kortus, *Chem. Commun.*, 2008, 52–54; (b) S. Piligkos, J. Bendix, H. Weihe, C. J. Milios and E. K. Brechin, *Dalton Trans.*, 2008, 2277–2284.
- 7 (a) V. Zerbib, F. Robert and P. Gouzerh, *J. Chem. Soc., Chem. Commun.*, 1994, 2179–2180; (b) P. Gouzerh and A. Proust, *Chem. Rev.*, 1998, **98**, 77–111.
- 8 (a) E. Ruiz, P. Alemany, S. Alvarez and J. Cano, *J. Am. Chem. Soc.*, 1997, **119**, 1297–1303; (b) E. Ruiz, S. Alvarez, J. Cano and V. Polo, *J. Chem. Phys.*, 2005, **123**, 164110; (c) E. Cremades, J. Cano, E. Ruiz, G. Rajaraman, C. J. Milios and E. K. Brechin, *Inorg. Chem.*, 2009, **48**, 8012–8019; (d) E. Cremades, T. Cauchy, J. Cano and E. Ruiz, *Dalton Trans.*, 2009, 5873–5878; (e) A. D. Becke, *J. Chem. Phys.*, 1993, **98**, 5648–5652; (f) A. Schaefer, C. Huber and R. Ahlrichs, *J. Chem. Phys.*, 1994, **100**, 5829–5835; (g) M. J. Frisch, *et al.*, *Gaussian03*, Gaussian, Inc, Pittsburgh, PA, 2003.
- 9 (a) A. J. M. Duisenberg, L. M. J. Kroon-Batenburg and A. M. M. Schreurs, *J. Appl. Crystallogr.*, 2003, **36**, 220; (b) G. M. Sheldrick, *Acta Crystallogr., Sect. A: Found. Crystallogr.*, 2008, **64**, 112–122.